Novel electron scattering experiment finds a small proton radius

W. Xiong[1], A. Gasparian[2], H. Gao[1], D. Dutta[3†], M. Khandaker[4], N. Liyanage[5], E. Pasyuk[6], C. Peng[1], X. Bai[5], L. Ye[3], K. Gnanvo[5], C. Gu[1], M. Levillain[2], X. Yan[1], D. W. Higinbotham[6], M. Meziane[1], Z. Ye[1,7], K. Adhikari[3], B. Aljawrneh[2], H. Bhatt[3], D. Bhetuwal[3], J. Brock[6], V. Burkert[6], C. Carlin[6], A. Deur[6], D. Di[5], J. Dunne[3], P. Ekanayaka[3], L. El-Fassi[3], B. Emmich[3], L. Gan[8], O. Glamazdin[9], M. L. Kabir[3], A. Karki[3], C. Keith[6], S. Kowalski[10], V. Lagerquist[11], I. Larin[12,13], T. Liu[1], A. Liyanage[14], J. Maxwell[6], D. Meekins[6], S. J. Nazeer[14], V. Nelyubin[5], H. Nguyen[5], R. Pedroni[2], C. Perdrisat[15], J. Pierce[6], V. Punjabi[16], M. Shabestari[3], A. Shahinyan[17], R. Silwal[10], S. Stepanyan[6], A. Subedi[3], V. V. Tarasov[12], N. Ton[5], Y. Zhang[1] and Z. W. Zhao[1]

Elastic electron-proton scattering ($e-p$) and the spectroscopy of hydrogen atoms are the two traditional methods used to determine the proton charge radius (r_p). About a decade ago, a new method using muonic hydrogen (μH) atoms [1] found a significant discrepancy with the compilation of all previous results [2], creating the "proton radius puzzle". Despite intensive world-wide experimental and theoretical efforts, the "puzzle" remains unresolved. In fact, a new discrepancy was reported between the two most recent spectroscopic measurements on ordinary hydrogen [3,4]. Here, we report on the PRad experiment, the first high-precision $e-p$ experiment since the emergence of the "puzzle". For the first time, a magnetic-spectrometer-free method was employed along with a windowless hydrogen gas target, which overcame several limitations of previous $e-p$ experiments and reached unprecedented small angles. Our result, r_p = 0.831 $\pm$ 0.007$_{\text{stat.}}$ $\pm$ 0.012$_{\text{syst.}}$ femtometer, is significantly smaller than the

[†]email:d.dutta@msstate.edu

last high-precision $e-p$ measurement [5] and the world average of all $e-p$ results [6]. The smaller r_p measured in our new $e-p$ experiment supports the small value found by the μH experiments. Additionally, the recently announced shift in the Rydberg constant [7], one of the best-known fundamental constants in physics, agrees with our finding.

The proton is the dominant ingredient of visible matter in the Universe. Consequently, determining the proton's basic properties such as its root-mean-square (RMS) charge radius, r_p, has attracted tremendous interest in its own right. Accurate knowledge of r_p is essential for the precise determination of fundamental constants such as the Rydberg constant (R_∞) [2]. It is also required for precise calculations of the energy levels and transition energies of the hydrogen (H) atom, for example, the Lamb shift. The extended proton charge distribution changes the Lamb shift by as much as 2% [1] in the case of μH atoms, where the electron in the H atom is replaced by a "heavier electron", the muon. The first principles calculation of r_p in the accepted theory of the strong interaction - Quantum Chromodynamics (QCD), is notoriously challenging and currently cannot reach the accuracy demanded by experiments, but, Lattice QCD calculations are on the cusp of becoming precise enough to be tested experimentally [8]. Therefore, precision measurement of r_p is critical for addressing the "proton radius puzzle" and also important for determining fundamental constants of physics and for testing lattice QCD.

Prior to 2010 the two methods used to measure r_p were: (i) $ep \to ep$ elastic scattering measurements, where the slope of the extracted electric form factor (G_E^p) down to zero 4-momentum transfer squared (Q^2), is proportional to r_p^2; and (ii) Lamb shift (spectroscopy) measurements of

"regular" H atoms, which, along with state-of-the-art calculations, were used to determine r_p. Although, the $e-p$ results can be somewhat less precise than the spectroscopy results, the value of r_p obtained from these two methods [2,5] mostly agreed with each other [9]. New results based on Lamb shift measurements in μH were reported for the first time in 2010. The Lamb shift in μH is several million times more sensitive to r_p because the muon is about 200 times closer to the proton than the electron in a H atom. To the surprise of both the nuclear and atomic physics communities, the two μH results [1,10] with their unprecedented, $<0.1\%$ precision, were a combined eight-standard deviations smaller than the average value from all previous experiments. This triggered the *"proton radius puzzle"* [11], unleashing intensive experimental and theoretical efforts aimed at resolving this "puzzle".

The discrepancy between r_p measured in H and μH atoms remains unresolved. Moreover, the two most recent H spectroscopy measurements disagree with each other [3,4], which has added a new dimension to and renewed the urgency of this problem. A fundamental difference between the $e-p$ and $\mu-p$ interactions, could be the origin of the discrepancy. However, there are abundant experimental constraints on any such "new physics", and yet models that resolve the puzzle with new force carriers have been proposed [11,12]. On the other hand, more mundane solutions continue to be explored, for example, the definition of r_p used in all three major experimental approaches has been rigorously shown to be consistent [13]. The effect of two-photon exchange on μH spectroscopy [14,15] and form factor nonlinearities in $e-p$ scattering [16–18] have also been examined. None of these studies could adequately explain the "puzzle" and have reinforced the need for additional high-precision measurements of r_p, using new experimental techniques with different

systematics.

The PRad collaboration at Jefferson Lab developed and performed a new $e-p$ experiment as an independent measurement of r_p to address this "puzzle". The PRad experiment, in contrast with previous $e-p$ experiments, was designed to use a magnetic-spectrometer-free, calorimeter based method [19]. The innovative design of the PRad experiment enabled three major improvements over previous $e-p$ experiments: (i) The large angular acceptance $(0.7^\circ - 7.0^\circ)$ of the hybrid calorimeter (HyCal) allowed for a large Q^2 coverage spanning two orders of magnitude $(2.1 \times 10^{-4} - 6 \times 10^{-2})\,(\mathrm{GeV/c})^2$, in the low Q^2 range. The single fixed location of HyCal eliminated the multitude of normalization parameters that plague magnetic spectrometer based experiments, where the spectrometer must be physically moved to many different angles to cover the desired range in Q^2. In addition, the PRad experiment reached extreme forward scattering angles down to 0.7° achieving the lowest Q^2 $(2.1 \times 10^{-4}\,(\mathrm{GeV/c})^2)$ in $e-p$ experiments, an order of magnitude lower than previously achieved. Reaching a lower Q^2 range is critically important since r_p is extracted as the slope of the measured $G_E^p(Q^2)$ at $Q^2 = 0$. (ii) The extracted $e-p$ cross sections were normalized to the well known quantum electrodynamics process - $e^-e^- \rightarrow e^-e^-$ Møller scattering from the atomic electrons $(e-e)$ - which was measured simultaneously with the $e-p$ within the same detector acceptance. This leads to a significant reduction in the systematic uncertainties of measuring the $e-p$ cross sections. (iii) The background generated from the target windows, one of the dominant sources of systematic uncertainty for all previous $e-p$ experiments, is highly suppressed in the PRad experiment.

Figure 1: The PRad experimental setup. A schematic layout of the PRad experimental setup in Hall B at Jefferson Lab, with the electron beam incident from the left. The key beam line elements are shown along with the window-less hydrogen gas target, the two-segment vacuum chamber and the two detector systems (see the Supplementary Material for the description of the target and individual detectors and the Method Summary for a brief overview).

The PRad experimental apparatus consisted of the following four main elements (Figure 1): (i) a 4 cm long, windowless, cryo-cooled hydrogen (H_2) gas flow target with a density of 2×10^{18} atoms/cm^2. It eliminated the beam background from the target windows and was the first such target used in $e - p$ experiments; (ii) the high resolution, large acceptance HyCal electromagnetic calorimeter [20]. The complete azimuthal coverage of HyCal for the forward scattering angles allowed simultaneous detection of the pair of electrons from $e - e$ scattering, for the first time in these types of measurements; (iii) one plane made of two high resolution $X - Y$ gas electron multiplier (GEM) coordinate detectors located in front of HyCal; and (iv) a two-section vacuum chamber spanning the 5.5 m distance from the target to the detectors.

The PRad experiment was performed in Hall B at Jefferson Lab in May-June of 2016, using 1.1 GeV and 2.2 GeV electron beams. The standard Hall B beam line, designed for low beam currents (0.1-50 nA), was used in this experiment. The incident electrons that scattered off the target protons and the Møller electron pairs, were detected in the GEM and HyCal detectors. The energy and position of the detected electron(s) was measured by HyCal, and the transverse ($X - Y$) position was measured by the GEM detector, which was used to assign the Q^2 for each detected

event. The GEM detector, with a position resolution of 72 μm, improved the accuracy of Q^2 determination. Furthermore, the GEM detector suppressed the contamination from photons generated in the target and other beam line materials; the HyCal is equally sensitive to electrons and photons while the GEM is mostly insensitive to neutral particles. The GEM detector also helped suppress the position dependent irregularities in the response of the electromagnetic calorimeter. A plot of the reconstructed energy versus the reconstructed angle for $e-p$ and $e-e$ events is shown in Figure 2 for the 2.2 GeV beam energy.

Figure 2: Event reconstruction. The reconstructed energy vs angle for $e-p$ and $e-e$ events for the electron beam energy of 2.2 GeV. The red and black lines indicate the event selection for $e-p$ and $e-e$, respectively. The angles $\leq 3.5^\circ$ are covered by the $PbWO_4$ crystals and the rest by the Pb-glass part of HyCal.

The background was measured periodically with an empty target cell. To mimic the residual gas in the beam line, H_2 gas at very low pressure was allowed in the target chamber during the empty target runs. The charge normalized $e-p$ and Møller yields from the empty target cell were used to effectively subtract the background contributions. The beam current was measured with the Hall-B Faraday cup with an uncertainty of $< 0.1\%$ [21]. Further, details on the background subtraction can be found in the Supplemental Material.

A comprehensive Monte Carlo simulation of the PRad setup was developed using the Geant4 toolkit [22]. The simulation consists of two separate event generators built for the $e-p$ and $e-e$

processes [23,24]. Inelastic $e-p$ scattering events were also included in the simulation using a fit [25] to the $e-p$ inelastic world data. The simulation included signal digitization and photon propagation which were critical for the precise reconstruction of the position and energy of each event in the HyCal. The details are described in the Supplementary Material.

Figure 3: The measured cross section and form factor. **(a)** The reduced cross section ($\sigma_{\text{reduced}} = \left(\frac{d\sigma}{d\Omega}\right)_{e-p} / \left[\left(\frac{d\sigma}{d\Omega}\right)_{\text{point-like}} \left(\frac{4M_p^2 E'}{(4M_p^2+Q^2)E}\right)\right]$, where E is the electron beam energy, E' is the energy of the scattered electron and M_p is the mass of the proton), for the PRad $e-p$ data. Dividing out the kinematic factor inside the parentheses, the reduced cross section is a linear combination of the electromagnetic form factors squared. The systematic uncertainties are shown as bands. **(b)** The G_E^p as a function of Q^2. The data points are normalized with the n_1 and n_2 parameters, for the 1.1 GeV and 2.2 GeV data separately. Statistical uncertainties are shown as error bars. Systematic uncertainties are shown as bands, for 1.1 GeV (red) and 2.2 GeV (blue). The solid black curve shows the $G_E(Q^2)$ from the fit to the function given by Eq. 1. Also shown are the fit from a previous $e-p$ experiment [5] for $r_p = 0.883(8)$ fm (green) and the calculation of Alarcon *et al.* [26] for $r_p = 0.844(7)$ fm (purple).

The $e-p$ cross sections were obtained by comparing the simulated and measured $e-p$ yield relative to the simulated and measured $e-e$ yield (see Supplementary Material for details). The extracted reduced cross section is shown in Figure 3 (a). The $e-p$ elastic cross section is related to G_E^p and the proton magnetic form factor (G_M^p) as per the Rosenbluth formula [19]. In the very low Q^2 region covered by the PRad experiment, the cross section is dominated by the contribution from

G_E^p. Thus, the uncertainty introduced from G_M^p is negligible. In fact, when using a wide variety of parametrizations for G_M^p [5,27–29], the extracted G_E^p varies by $\sim 0.2\%$ at $Q^2 = 0.06\ (\mathrm{GeV/c})^2$, the largest Q^2 accessed by the PRad experiment, and $< 0.01\%$ in the $Q^2 <\ 0.01\ (\mathrm{GeV/c})^2$ region. The largest variation in r_p arising from the choice of G_M^p parametrization is 0.001 fm. The $G_E^p(Q^2)$ extracted from our data is shown in Figure 3 (b), where the Kelly parametrization for G_M^p [27] was used.

The slope of $G_E^p(Q^2)$ as $Q^2 \rightarrow 0$ is proportional to r_p^2. A common practice is to fit $G_E^p(Q^2)$ to a functional form and to obtain r_p by extrapolating to $Q^2 = 0$. However, each functional form truncates the higher-order moments of $G_E^p(Q^2)$ differently and introduces a model dependence which can bias the determination of r_p. It is critical to choose a robust functional form that is most likely to yield an unbiased estimation of r_p given the uncertainties in the data, and test the chosen functional form over a broad range of parametizations of $G_E^p(Q^2)$ [30]. To simultaneously minimize the possible bias in the radius extraction and the total uncertainty, various functional forms were examined for their robustness in reproducing an input r_p used to generate a mock data set that had the same statistical uncertainty as the PRad data. The robustness quantified as the root mean square error (RMSE) is defined as RMSE $= \sqrt{(\delta R)^2 + \sigma^2}$, where δR is the bias or the difference between the input and extracted radius and σ is the statistical variation of the fit to the mock data [30]. These studies show [30] (see Supplementary Material) that consistent results with the least uncertainties can be achieved when using the multi-parameter Rational-function (referred to as Rational (1,1)):

$$f(Q^2) = nG_E(Q^2) = n\frac{1 + p_1 Q^2}{1 + p_2 Q^2}, \tag{1}$$

where n is the floating normalization parameter, and the charge radius is given by $r_p = \sqrt{6(p_2 - p_1)}$.

The $G_E^p(Q^2)$ extracted from the 1.1 GeV and 2.2 GeV data were fitted simultaneously using the Rational (1,1) function. Independent normalization parameters n_1 and n_2 were assigned for 1.1 and 2.2 GeV data respectively, to allow for differences in normalization uncertainties, but the Q^2 dependence was identical. The parameters obtained from fits to the Rational (1,1) function are: $n_1 = 1.0002 \pm 0.0002_{\text{stat.}} \pm 0.0020_{\text{syst.}}$, $n_2 = 0.9983 \pm 0.0002_{\text{stat.}} \pm 0.0013_{\text{syst.}}$, and $r_p = 0.831 \pm 0.007_{\text{stat.}} \pm 0.012_{\text{syst.}}$ fm. The Rational (1,1) function describes the data very well, with a reduced χ^2 of 1.3 when considering only the statistical uncertainty. The values of r_p for a variety of functional forms fitted to the PRad data are shown in Supplementary Figure S15.

To determine the systematic uncertainty in r_p, a Monte Carlo technique was used to randomly smear the cross section and $G_E(Q^2)$ data points for each known source of systematic uncertainty. The r_p was extracted from the smeared data and the process is repeated 100,000 times. The RMS of the resulting distribution of r_p is recorded as the systematic uncertainty. The dominant systematic uncertainties of r_p are the Q^2 dependent ones which primarily affect the lowest-Q^2 data: the Møller radiative corrections, the background subtraction for the 1.1 GeV data, and event selection. The uncertainty of r_p arising from the finite Q^2 range and the extrapolation to Q^2 = 0, was investigated by varying the Q^2 range of the mock data set as part of the robustness study of the Rational (1,1) function [30]. This uncertainty was found to be much smaller than the relative statistical uncertainty of 0.8%. The total systematic relative uncertainty on r_p was found to be 1.4%, and is detailed in Supplementary Table 1, and described in the Supplemental Material.

The r_p obtained using the Rational (1,1) function is shown in Figure 4, with statistical and

systematic uncertainties summed in quadrature. Our result obtained from Q^2 down to an unprecedented 2.1×10^{-4} (GeV/c)^2, is about 3-standard deviations smaller than the previous high-precision electron scattering measurement [5], which was limited to higher Q^2 (> 0.004 (GeV/c)^2). On the other hand, our result is consistent with the μH Lamb shift measurements[1,10], and also the recent 2S-4P transition frequency measurement using ordinary H atoms [3]. Given that the lowest Q^2 reached in the PRad experiment is an order of magnitude lower than the previous $e-p$ experiments, and the careful control of systematic effects, our result indicates that the proton is indeed smaller than the previously accepted value from $e-p$ measurements. Our result does not support any fundamental difference between the $e-p$ and $\mu-p$ interactions and is consistent with the shift in the Rydberg constant announced by CODATA [7].

Figure 4: The proton charge radius. The r_p extracted from the PRad data, shown along with the other measurements of r_p since 2010 and the CODATA recommended values.The PRad result is 2.7-σ smaller than the CODATA recommended value for $e-p$ experiments [6].

The PRad experiment is the first $e-p$ experiment to cover a two orders of magnitude span of Q^2, in one setting. The experiment also exploited the simultaneous detection of $e-p$ and $e-e$ scattering to achieve superior control of systematic uncertainties, which were by design different from previous $e-p$ experiments. Further, the extraction of r_p by employing functional forms with validated robustness is another strength of this result. Our result introduces a large discrepancy with contemporary precision $e-p$ experiments. On the other hand, the results also imply that there is consistency between proton charge radii obtained from $e-p$ scattering on regular

hydrogen and spectroscopy of muonic hydrogen [1,10] and that the value of r_p is consistent with the recently updated CODATA value [7]. The PRad experiment demonstrates the clear advantages of the calorimeter based method for extracting r_p from $e - p$ experiments and points to further possible improvements in the accuracy of this method. It also validates the recently announced shift in the Rydberg constant [7], which has profound consequences, given that the Rydberg constant is one of the most precisely known constants of physics.

1. Pohl, R. *et al.*, "The size of the proton," *Nature* **466**, 213–217 (2010).

2. Mohr, P. J., Taylor, B. N. & Newell, D. B. "CODATA recommended values of the fundamental physical constants: 2006," *Rev. Mod. Phys.* **80**, 633–730 (2008).

3. Beyer, A. *et al.*, "The Rydberg constant and proton size from atomic hydrogen," *Science* **358**, 79–86 (2017).

4. Fleurbaey, H. *et al.*, "New Measurement of the 1S-3S Transition Frequency of Hydrogen: Contribution to the Proton Charge Radius Puzzle," *Phys. Rev. Lett.* **120**, 183001 (2018).

5. Bernauer, J. C. *et al.*, "High-Precision Determination of the Electric and Magnetic Form Factors of the Proton," *Phys. Rev. Lett.* **105**, 242001 (2010).

6. Mohr, P. J., Newell, D. B. & Taylor, B. N. 'CODATA recommended values of the fundamental physical constants: 2014," *J. of Phys. and Chem. Ref. Data* **45**, 043102 (2016).

7. Mohr, P. J., Newell, D. B. & Taylor, B. N. 'CODATA recommended values of the fundamental physical constants: 2018." `http://physics.nist.gov/constants` (2019).

8. Hasan, N. *et al.*, "Computing the Nucleon Charge and Axial Radii Directly at $Q^2 = 0$ in Lattice QCD," *Phys. Rev. D* **97**, 034504 (2018).

9. Mohr, P. J., Taylor, B. N. & Newell, D. B. "CODATA recommended values of the fundamental physical constants: 2010," *Rev. Mod. Phys.* **84**, 1527–1605 (2012).

10. Antognini, A. *et al.*, "Proton structure from the measurement of 2S-2P transition frequencies of muonic hydrogen," *Science* **339**, 417–420 (2013).

11. Carlson, C. E. "The Proton Radius Puzzle," *Prog. Part. Nucl. Phys.* **82**, 59–77 (2015).

12. Liu, Y. S. & Miller, G. A. "Validity of the Weizsäcker-Williams approximation and the analysis of beam dump experiments: Production of an axion, a dark photon, or a new axial-vector boson," *Phys. Rev. D* **96**, 016004 (2017).

13. Miller, G.A. "Defining the proton radius: A unified treatment,"*Phys. Rev. C* **99**, 035202 (2019).

14. Miller, G. A. "Proton polarizability contribution: Muonic hydrogen Lamb shift and elastic scattering," *Phys. Lett. B* **718**, 1078–1082 (2013).

15. Antognini, A. *et al.*, "Theory of the 2S–2P Lamb shift and 2S hyperfine splitting in muonic hydrogen," *Annals Phys.* **331**, 27–145 (2013).

16. Lee, G., Arrington, J. R. & Hill, R. J. "Extraction of the proton radius from electron-proton scattering data," *Phys. Rev. D* **92**, 013013 (2015).

17. Higinbotham, D. W. *et al*, "Proton Radius from Electron Scattering Data," *Phys. Rev. C* **93**, 055207 (2016).

18. Griffioen, K., Carlson, C. & Maddox, S. "Consistency of electron scattering data with a small proton radius,", *Phys. Rev. C* **93**, 065207 (2016).

19. Gasparian, A., Khandakar, M., Gao, H., Dutta, D. *et al.*, "A proposal for Jefferson Laboratory: High Precision Measurement of the Proton Charge Radius." `https://www.jlab.org/exp_prog/proposals/12/c12-11-106.pdf` (2011). JLab PAC39 proposal C12-11-106.

20. Gasparian, A. "A High Performance Hybrid Electromagnetic Calorimeter at Jefferson Lab." In Cecchi, C., Cenci, P., Lubrano, P. & Pepe, M. (eds.) *Proc. XI Int. Conf. Calorim. Part. Phys.*, 109–115 (World Scientific, Singapore, 2005).

21. Mecking, B. *et al.*, "The CEBAF Large Acceptance Spectrometer (CLAS)," *Nucl. inst. and Meth. A*, **503** 513–553 (2003).

22. Agostinelli, S. *et al.*, "GEANT4: A Simulation toolkit," *Nucl. Inst. and Meth. A* **506**, 250–303 (2003).

23. Akushevich, I., Gao, H., Ilyichev, A. & Meziane, M. "Radiative corrections beyond the ultra relativistic limit in unpolarized ep elastic and Møller scatterings for the PRad Experiment at Jefferson Laboratory," *Eur. Phys. J. A* **51**, 1 (2015).

24. Gramolin, A. V. *et al.*, "A new event generator for the elastic scattering of charged leptons on protons," *J. Phys. G* **41**, 115001 (2014).

25. Christy, M. E. & Bosted, P. E. "Empirical fit to precision inclusive electron-proton cross-sections in the resonance region," *Phys. Rev. C* **81**, 055213 (2010).

26. Alarcon, J. M., Higinbotham, D. W., Weiss, C. & Ye, Z., "Proton Charge Radius from Electron Scattering Data Using Dispersively Improved Chiral Effective Field Theory," *Phys. Rev. C* **99**, 044303 (2019).

27. . Kelly, J. J"Simple parametrization of nucleon form factors," *Phys. Rev. C* **70**, 068202 (2004).

28. Venkat, S., Arrington, J., Miller, G. A. & Zhan, X. "Realistic Transverse Images of the Proton Charge and Magnetic Densities," *Phys. Rev. C* **83**, 015203 (2011).

29. Higinbotham, D. W. & McClellan, R. E. "How Analytic Choices Can Affect the Extraction of Electromagnetic Form Factors from Elastic Electron Scattering Cross Section Data," arXiv:1902.08185 (2018).

30. Yan, X. *et al.*, "Robust extraction of the proton charge radius from electron-proton scattering data," *Phys. Rev. C* **98**, 025204 (2018).

Figure Captions

Figure 1: The PRad experimental setup. A schematic layout of the PRad experimental setup in Hall B at Jefferson Lab, with the electron beam incident from the left. The key beam line elements are shown along with the window-less hydrogen gas target, the two-segment vacuum chamber and the two detector systems (see the Supplementary Material for the description of the target and individual detectors and the Method Summary for a brief overview).

Figure 2: Event reconstruction. The reconstructed energy vs angle for $e-p$ and $e-e$ events for the electron beam energy of 2.2 GeV. The red and black lines indicate the event selection for $e-p$ and $e-e$, respectively. The angles $\leq 3.5^\circ$ are covered by the $PbWO_4$ crystals and the rest by the Pb-glass part of HyCal.

Figure 3:The measured cross section and form factor. **(a)** The reduced cross section ($\sigma_{\text{reduced}} = \left(\frac{d\sigma}{d\Omega}\right)_{e-p} / \left[\left(\frac{d\sigma}{d\Omega}\right)_{\text{point-like}} \left(\frac{4M_p^2 E'}{(4M_p^2+Q^2)E}\right)\right]$, where E is the electron beam energy, E' is the energy of the scattered electron and M_p is the mass of the proton), for the PRad $e-p$ data. Dividing out the kinematic factor inside the parentheses, the reduced cross section is a linear combination of the electromagnetic form factors squared. The systematic uncertainties are shown as bands. **(b)** The G_E^p as a function of Q^2. The data points are normalized with the n_1 and n_2 parameters, for the 1.1 GeV and 2.2 GeV data separately. Statistical uncertainties are shown as error bars. Systematic uncertainties are shown as bands, for 1.1 GeV (red) and 2.2 GeV (blue). The solid black curve shows

the $G_E(Q^2)$ from the fit to the function given by Eq. 1. Also shown are the fit from a previous $e-p$ experiment [5] for $r_p = 0.883(8)$ fm (green) and the calculation of Alarcon *et al.* [26] for $r_p = 0.844(7)$ fm (purple).

Figure 4: The proton charge radius. The r_p extracted from the PRad data, shown along with the other measurements of r_p since 2010 and the CODATA recommended values.The PRad result is 2.7-σ smaller than the CODATA recommended value for $e-p$ experiments [6].

Affiliations

[1]*Duke University and Triangle Universities Nuclear Laboratory, Durham, NC 27708, USA*

[2]*North Carolina A & T State University, Greensboro, NC 27424, USA*

[3]*Mississippi State University, Mississippi State, MS 39762, USA*

[4]*Idaho State University, Pocatello, ID 83209, USA*

[5]*University of Virginia, Charlottesville, VA 22904, USA*

[6]*Thomas Jefferson National Accelerator Facility, Newport News, VA 23606, USA*

[7]*Argonne National Lab, Lemont, IL 60439, USA*

[8]*University of North Carolina, Wilmington, NC 28402, USA*

[9]*Kharkov Institute of Physics and Technology, Kharkov 61108, Ukraine*

[10]*Massachusetts Institute of Technology, Cambridge, MA 02139, USA*

[11] *Old Dominion University, Norfolk, VA 23529 , USA*

[12] *Alikhanov Institute for Theoretical and Experimental Physics NRC "Kurchatov Institute", Moscow, 117218, Russia*

[13] *University of Massachusetts, Amherst, MA 01003, USA*

[14] *Hampton University, Hampton, VA 23669, USA*

[15] *College of William and Mary, Williamsburg, VA 23185, USA*

[16] *Norfolk State University, Norfolk, VA 23504, USA*

[17] *Yerevan Physics Institute, Yerevan 0036, Armenia*

Acknowledgements

This work was funded in part by the U. S. National Science Foundation (NSF MRI PHY-1229153) and by the U.S. Department of Energy (Contract No. DE-FG02-03ER41231), including contract No. DE-AC05-06OR23177 under which Jefferson Science Associates, LLC operates Thomas Jefferson National Accelerator Facility. We wish to thank the staff of Jefferson Lab for their vital support throughout the experiment. We are also grateful to all granting agencies for providing funding support to the authors throughout this project. We acknowledge fruitful discussions about radiative corrections with A. Afanasev, I. Akushevich, A. V. Gramolin and O. Tomalak. We thank S. Danagoulian for helping restore the light monitoring system of HyCal. We also thank S. Javalkar for help with a beam halo study.

Notice to Publisher: Authored by Jefferson Science Associates, LLC under U.S. DOE Contract No. DE-AC05-06OR23177. The U.S. Government retains a non-exclusive, paid-up, irrevocable, world-wide license to publish or reproduce this manuscript for U.S. Government purposes.

Competing Interests The authors declare that they have no competing financial interests.

Correspondence Correspondence and requests for materials should be addressed to D. Dutta (email: d.dutta@msstate.edu).

Author contributions statement

A.G. is the spokesperson of the experiment. H.G., D.D., and M.K. are co-spokespersons of the experiment. A.G. developed the initial concepts of the experiment. A.G., H.G., D.D, and M.K designed and proposed the experiment. The entire PRad collaboration constructed the experiment and worked on the data collection. The COMSOL simulation of the target was built by Y.Z. The Monte Carlo simulation was built and validated by C.P., C.G., W.X., X.B. with input from numerous other members of the collaboration. Calibrations were carried out by W.X., M.L., X.B., C.P., L.Y., X.Y. with input from I.L. Analysis software tools were developed by C.P, with input from X.B., M.L., I.L., L.Y., W.X. and X.Y. The data analysis was carried out by W.X., C.P., X.B., M.L., C.G. with input from A.G, H.G., D.D., M.K, N.L., E.P., X.Y., D.W.H., L.Y.and M.L.K. All authors reviewed the manuscript.

Data Availability

The raw data from this experiment are archived in Jefferson Laboratory's mass storage silo.

Code Availability

All computer codes used for data analysis and simulation are archived in Jefferson Laboratory's mass storage silo.

Methods Summary

The PRad experiment was conducted with 1.1 GeV and 2.2 GeV electron beams from the CEBAF accelerator incident on cold hydrogen atoms flowing through a windowless target cell. The scattered electrons after traversing the vacuum chamber were detected in the gas electron multiplier (GEM) and the HyCal electromagnetic calorimeter. They included electrons from elastic $e-p$ scattering and $e-e$ Møller scattering processes. The transverse $(X-Y)$ positions measured by the GEM detector were used to calculate the Q^2 for each event. The $e-p$ and $e-e$ yields were obtained by using appropriate cuts on the energy deposited in HyCal and the reconstructed angle. The $e-p$ and $e-e$ yields were binned as a function of Q^2. A comprehensive Monte Carlo simulation of the PRad experiment was used to extract the next-to-leading order $e-p$ cross section from the experimental yields. The $e-p$ cross sections were obtained by comparing the simulated and measured $e-p$ yield relative to the simulated and measured Møller yield. The G_E^p was extracted from the $e-p$ cross section using the Rosenbluth formula and a parametrization of G_M^p. The

proton charge radius, r_p, was obtained from the extracted $G_E^p(Q^2)$ by fitting to a Rational (1,1) functional form and extrapolating to $Q^2 = 0$. The Rational (1,1) functional form was shown to be the most robust function for radius extraction from the PRad data, giving consistent results with the least uncertainties.

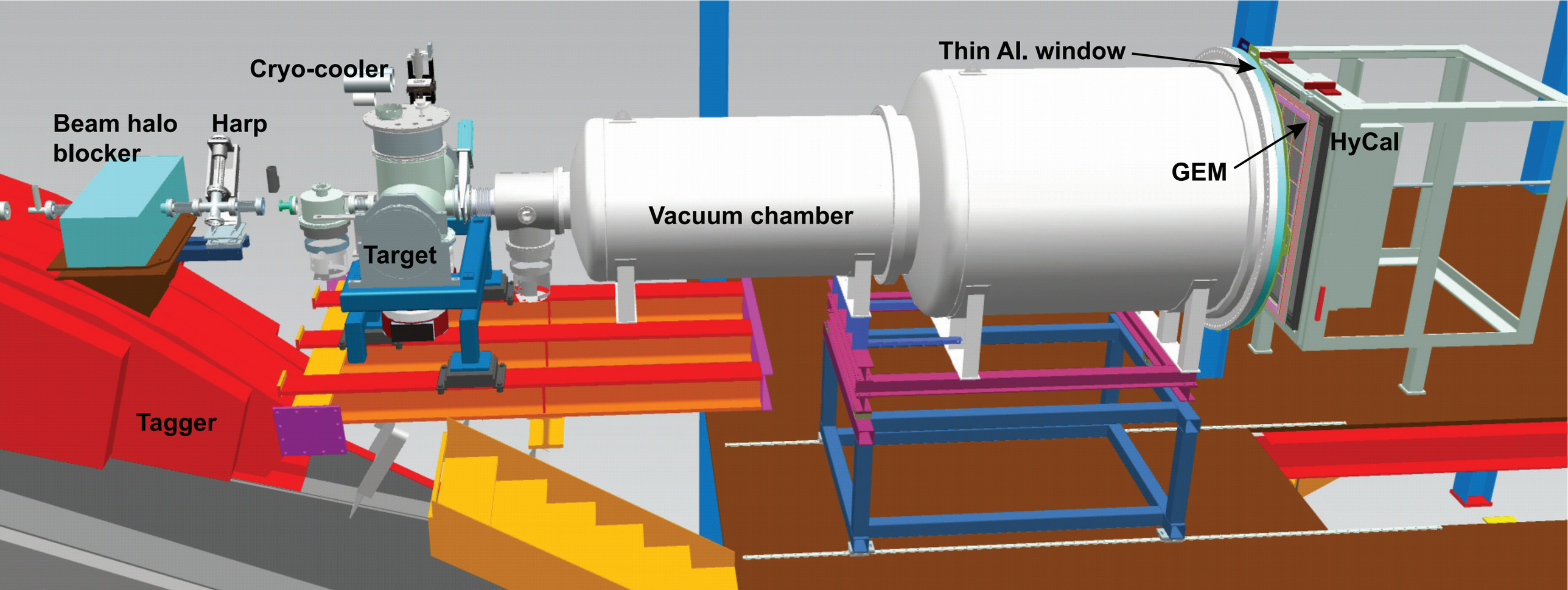
Cryo-cooler
Beam halo blocker
Harp
Target
Tagger
Vacuum chamber
Thin Al. window
GEM
HyCal

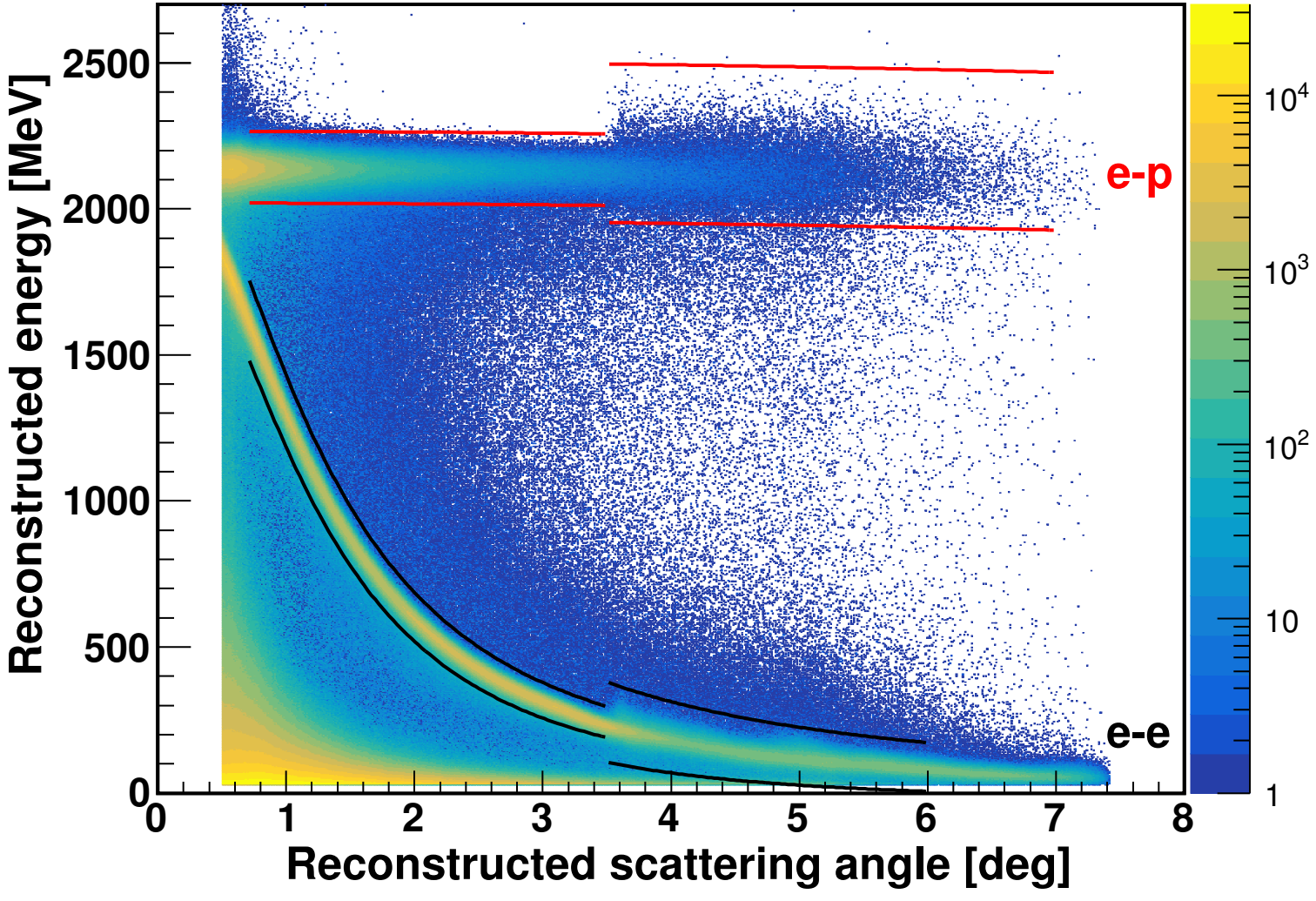
Reconstructed energy [MeV]
2500
2000
1500
1000
500
0
0
1
2
3
4
5
6
7
8
Reconstructed scattering angle [deg]
e-p
e-e
10^4
10^3
10^2
10
1

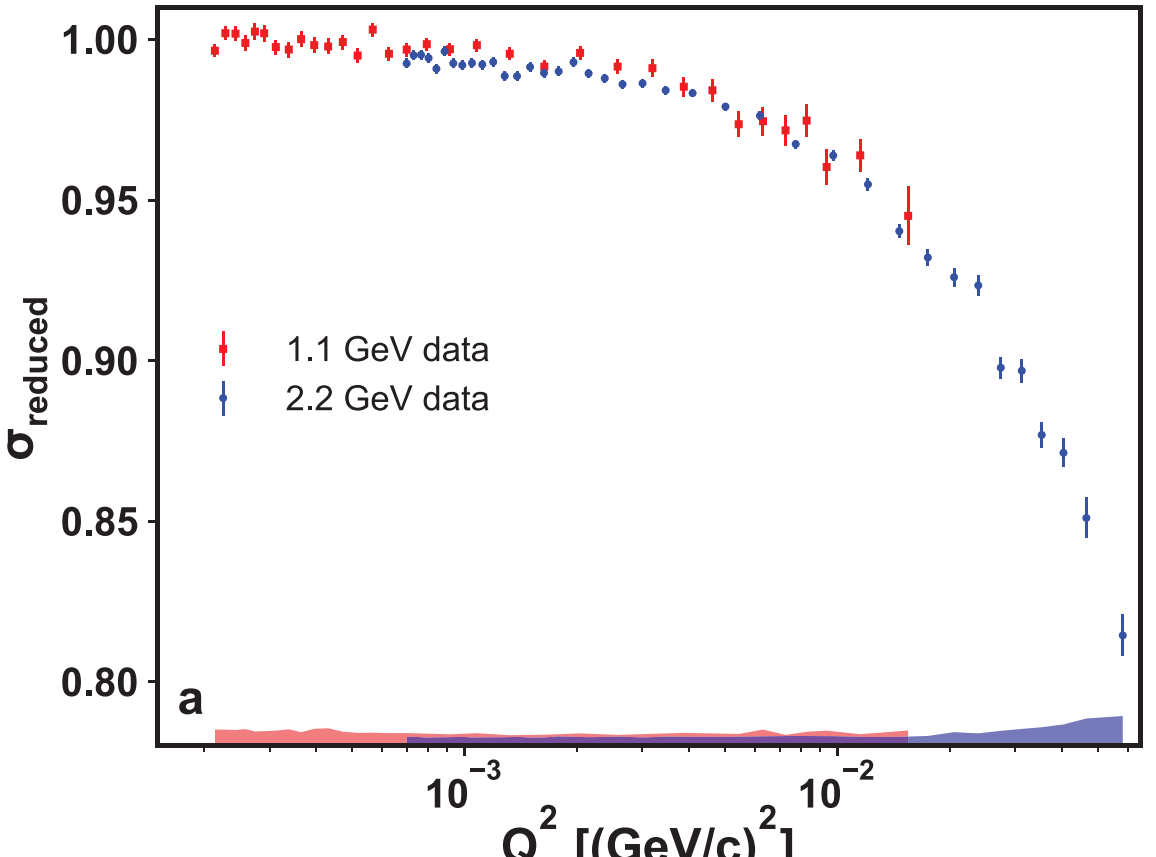
1.00
0.95
0.90
0.85
0.80
$\sigma_{reduced}$
1.1 GeV data
2.2 GeV data
a
10^{-3}
10^{-2}
Q^2 [(GeV/c)^2]

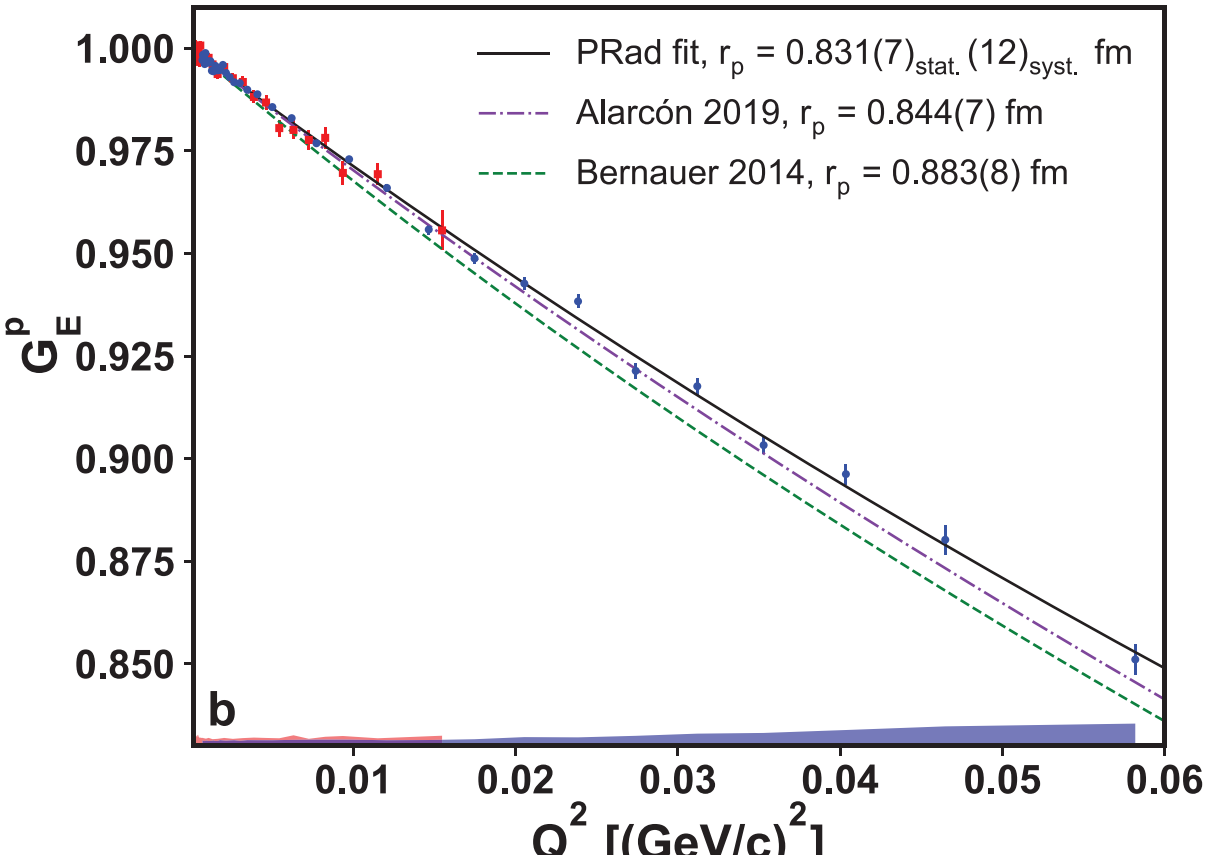
1.000
0.975
0.950
0.925
0.900
0.875
0.850
G_E^p
PRad fit, r_p = 0.831(7)$_{stat.}$ (12)$_{syst.}$ fm
Alarcón 2019, r_p = 0.844(7) fm
Bernauer 2014, r_p = 0.883(8) fm
b
0.01
0.02
0.03
0.04
0.05
0.06
Q^2 [(GeV/c)^2]

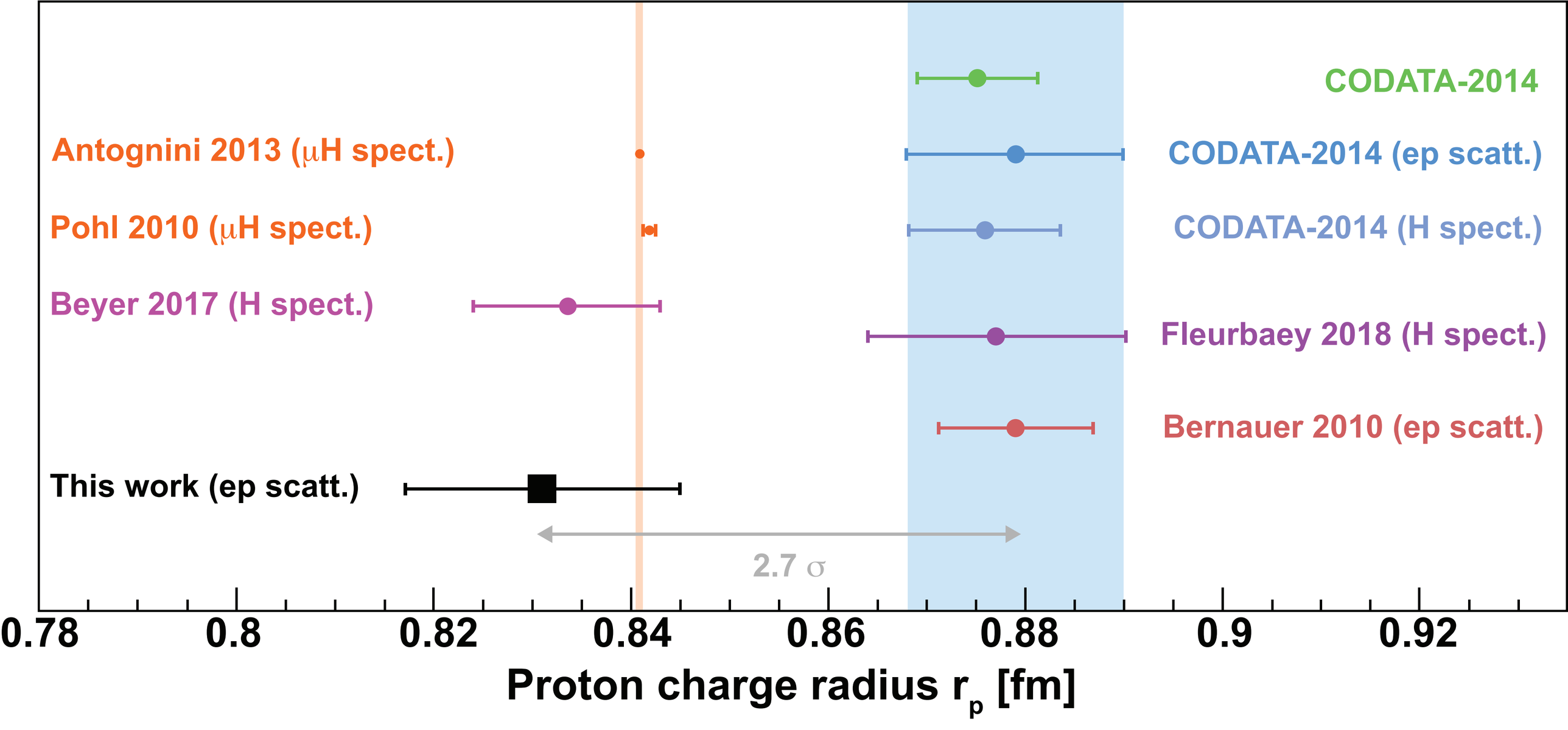
CODATA-2014
Antognini 2013 (μH spect.)
CODATA-2014 (ep scatt.)
Pohl 2010 (μH spect.)
CODATA-2014 (H spect.)
Beyer 2017 (H spect.)
Fleurbaey 2018 (H spect.)
Bernauer 2010 (ep scatt.)
This work (ep scatt.)
2.7 σ
0.78
0.8
0.82
0.84
0.86
0.88
0.9
0.92
Proton charge radius r_p [fm]